

Polarization and Charge Transfer in the Hydration of Chloride Ions

Zhen Zhao and David M. Rogers*
*Department of Chemistry, University of Cincinnati,
Cincinnati, OH 45221-0172*

Thomas L. Beck†
*Departments of Chemistry and Physics,
University of Cincinnati,
Cincinnati, OH 45221-0172*
(Dated: February 7, 2020)

A theoretical study of the structural and electronic properties of the chloride ion and water molecules in the first hydration shell is presented. The calculations are performed on an ensemble of configurations obtained from molecular dynamics simulations of a single chloride ion in bulk water. The simulations utilize the polarizable AMOEBA force field for trajectory generation, and MP2-level calculations are performed to examine the electronic structure properties of the ions and surrounding waters in the external field of more distant waters. The ChelpG method is employed to explore the effective charges and dipoles on the chloride ions and first-shell waters. The Quantum Theory of Atoms in Molecules (QTAIM) is further utilized to examine charge transfer from the anion to surrounding water molecules. The clusters extracted from the AMOEBA simulations exhibit high probabilities of anisotropic solvation for chloride ions in bulk water. From the QTAIM analysis, 0.2 elementary charges are transferred from the ion to the first-shell water molecules. The default AMOEBA model overestimates the average dipole moment magnitude of the ion compared with the estimated quantum mechanical value. The average magnitude of the dipole moment of the water molecules in the first shell treated at the MP2 level, with the more distant waters handled with an AMOEBA effective charge model, is 2.67 D. This value is close to the AMOEBA result for first-shell waters (2.72 D) and is slightly reduced from the bulk AMOEBA value (2.78 D). The magnitude of the dipole moment of the water molecules in the first solvation shell is most strongly affected by the local water-water interactions and hydrogen bonds with the second solvation shell, rather than by interactions with the ion.

PACS numbers: 82.60.Lf, 87.16.A-, 61.20.Ja, 64.70.qd, 64.75.Bc

I. INTRODUCTION

Fundamental studies of the thermodynamic and structural properties of ions in water and near proteins are important for understanding a wide range of chemical and biological phenomena. For example, in the central nervous system, ion-coupled membrane transporters regulate signaling by utilizing the electrochemical potential of specific ions to pump organic substrates and amino acids across the cell membrane [1, 2, 3]. As another example, chloride transporters exchange two chloride ions for one proton during the transport cycle [4, 5, 6]. To gain more insight into the mechanism, specificity, and function of these transporters, the binding properties of specific ions to the transporters and the ion hydration process in bulk water need to be characterized.

The hydration of atomic and molecular ions has been the focus of intensive research for over 100 years. More recently, specific ion effects have resurfaced in diverse fields [7], including hydration free energies, ion activities, surface tension increments, bubble interactions, colloid interactions, biological membrane multilayer swelling [8], and polymer phase equilibria [9], to name several examples. Such specificity requires theoretical treatments that go beyond simple dielectric models. Specific interactions at the molecular level are involved, and that specificity can lead to dramatic changes in bulk properties when one ion is substituted with another [8]. It has been argued that ion specificity is a central problem in connecting physical science to biological systems, and that the connection has not been fully made so far [10].

Calculation of the solvation and binding properties of an ion in water and near proteins for a classical model is

* Present address: Sandia National Laboratories, Albuquerque, NM 87185

†Electronic address: thomas.beck@uc.edu

now routine on modern workstations. The accuracy of these calculations depends sensitively on the classical model potential used, however. In the same spirit as Doren, Wood, and coworkers [11, 12, 13, 14], we are interested in incorporating quantum mechanical calculations in the study of the thermodynamics of ions in water and near proteins. The basic idea in Refs. [11, 12, 13, 14] is to perform classical simulations, obtain the free energy from those classical simulations, and then use the classical configurations coupled with statistical mechanical perturbation theory to correct those free energies towards the quantum result. This method is less expensive than a direct *ab initio* molecular dynamics (AIMD) quantum simulation [15, 16, 17, 18] since it uses a classical simulation to generate configurations for thermal averages. It is also more accurate than a classical simulation since it can in principle represent the electronic properties near the ions from first principles.

As a first step, here we study the aqueous solvation structures of the chloride ion in bulk water by utilizing the classical polarizable AMOEBA force field simulations and then by performing detailed quantum mechanical calculations on local solvation clusters extracted from the classical simulations. The cluster refers to the chloride ion and the coordinating water molecules in the first solvation shell, including interactions with more distant waters at the AMOEBA level. The polarization of the water molecules and ions in their solvation environment is explored by analyzing charges and dipoles generated from the charge distribution in the quantum mechanical model. Higher-level electronic structure methods (MP2 level) are employed to include electron correlation effects at a modest level of accuracy. Also, the first-shell water polarization is studied as a function of the cluster size. The present approach allows efficient calculation of configurational averages for an accurate QM/MM model. This paper is part of a series developing and exploiting computational methods for calculating the electronic and thermodynamic properties of ions in water [19, 20]. Future work will focus on ion binding in proteins.

The paper is organized as follows. We next discuss the classical and quantum computational approaches employed for the study of local hydration structure. The results of the calculations are then presented, followed by our conclusions and discussion of implications for simulations of ion hydration and future research directions.

II. THEORETICAL AND COMPUTATIONAL METHODS

In this section, we present our approach for studying the electronic structural properties of the anion solvation shell.

A. Classical Simulation of the Chloride Ion in Water

The molecular dynamics (MD) trajectories were generated using the polarizable AMOEBA force field [21, 22, 23] as implemented in the AMBER package [24]. The AMOEBA force field has been shown to reproduce the expected dipole moment, dielectric constant, and energetics of bulk water from the gas phase to the bulk phase [22] and over a wide range of temperatures and pressures [21]. In addition, this force field has been extended to include ion-water interactions, and excellent results for ion hydration free energies have been obtained [25].

The simulated bulk system consists of a single Cl^- ion and 215 water molecules. The simulations were performed using a timestep of 1.25 fs. Configurations were saved every 0.5 ps for later analysis. Periodic boundary conditions were applied in all three dimensions. Long-range electrostatic interactions were handled using the PME algorithm [26] with a real-space cutoff of 8 Å. The nonbonded interactions were truncated at 10 Å. The temperature was maintained at 300 K using Langevin dynamics with a collision frequency of 5ps^{-1} . The pressure was maintained at 1.0 atm using the isotropic position scaling scheme with a pressure relaxation time of 2.0 ps. The cubic simulation box was allowed to scale in size isotropically in order to maintain constant pressure. The system was equilibrated for 120 ps (the system density was seen to converge within the first 20 ps), and then a production run of 500ps was performed for further analysis.

B. Electronic Structure Calculations

The geometries of the anion-water clusters were extracted from the AMOEBA molecular dynamics trajectories for the subsequent electronic structure calculations. The clusters for a given system configuration consisted of the chloride ion and all waters that satisfied a hydrogen-bonding condition discussed below. There is of course no guarantee that these configurations accurately represent the solvation environment at the quantum level. In another paper [20], we have found that anion solvation anisotropy in classical polarizable force field simulations is significantly affected by the polarizability of the anion. In addition, we found that the AMOEBA model over-polarizes the chloride ion by roughly a factor of 2 relative to AIMD simulations [17, 20]. Thus we performed simulations both with the default AMOEBA chloride ion polarizability (4Å^3) and with the polarizability reduced by a factor of 2. While the solvation anisotropy

TABLE I: The effect of basis set on the dipole moment of an isolated water molecule calculated at the MP2 level.

| Basis Set | μ_{SCF} (Debyes) |
|------------------|----------------------|
| 6-31G | 2.54220 |
| 6-31G** | 2.09900 |
| 6-31+G* | 2.33330 |
| 6-31+G** | 2.24850 |
| 6-31++G** | 2.23730 |
| 6-31++G(2df,p) | 2.03720 |
| 6-31++G(3df,2p) | 1.88510 |
| 6-311++G(3df,2p) | 1.93650 |
| cc-pvtz | 1.92060 |
| aug-cc-pvdz | 1.86620 |
| aug-cc-pvtz | 1.85120 |

decreases with the lower polarizability value, the results for water dipole magnitudes and charge transfer computed quantum mechanically did not substantially change; as expected, the ion dipoles from the AMOEBA model decreased substantially to 62% of the computed average from the default simulation, and the estimated quantum mechanical ion dipoles decreased slightly due to the reduced hydration anisotropy (below).

The electronic structure calculations were performed at the 2nd-order perturbation theory level. The MP2 calculations were performed with the Gaussian 03 package [27] using augmented correlation-consistent polarized valence basis sets of double ζ quality (aug-cc-pVDZ) [28]. This basis set has been shown to yield accurate molecular electrostatic interaction energies [29] and charge transfer estimates compared with experiment [30]. The total energy was converged to a precision of 10^{-8} Hartrees. The charge distribution was investigated using the same method and basis set.

Table I displays the convergence of the MP2-level single-water dipole moments with increasingly accurate basis sets. The experimental geometry for the monomer [$r[\text{OH}]=0.9572$, $\angle\text{HOH} = 104.52^\circ$] was assumed [31]. The dipole moment of the monomer calculated with Dunning’s correlation consistent basis sets augmented with diffuse functions (aug-cc-pvdz and aug-cc-pvtz) shows the best agreement with the experimental result (1.85-1.86 D) [32]. We chose the aug-cc-pvdz basis set [28] for both efficiency and high quality results [29, 30].

There exists a variety of methods available for estimating atomic charges and dipoles from the electron density. One approach is to obtain effective charges from the Electrostatic Potential (ESP) by fitting charges (and perhaps point dipoles) to match the ESP computed at the quantum level; points within the van der Waals radii of the atoms in the molecule or cluster are excluded from the fit. The ChelpG method is a widely used numerical implementation of this approach [33]. The ESP methods have been applied in Monte Carlo simulations [34], molecular dynamics simulations [35, 36], molecular modeling [37], and other applications [38]. Besides the ESP methods, atomic charges can be determined more rigorously by Bader’s Quantum Theory of Atoms in Molecules [39, 40] (QTAIM). The QTAIM approach provides an unambiguous quantum definition of an atom within a molecule based on the zero-flux surface of the electron density surrounding the atom (or ion).

Studies have shown that the ChelpG method is capable of providing accurate estimates of molecular dipoles [41, 42, 43] and charge transfer effects [30]. The results we present below show that the ChelpG-estimated anion and first-shell water dipoles are physically consistent with other quantum methods such as AIMD simulations. The estimated net effective charge on the chloride ion is somewhat ambiguous from the ChelpG calculations, however, since a single charge is employed in the ESP fitting to represent the complicated and diffuse charge distribution of the anion. Concerns have also been raised related to applying the ChelpG method to densely packed systems involving charged interactions occurring within the van der Waals radii of the interacting species [42, 44]; recent work has shown, however, that accurate estimates of effective atomic charges can be obtained for dense ionic systems in comparison with an alternative robust charge placement (Blöchl) algorithm [36, 45]. Our ChelpG cluster studies involve the chloride ion and up to 6 water molecules, and the ion is most often near the surface of the cluster. Thus there are not many ‘buried’ atoms in the ESP fitting, a point of concern in previous studies [36]. In light of these ambiguities, we further analyzed possible charge transfer effects with the QTAIM method by computing the distribution of instantaneous anion charges within the surface centered on the chloride ion and specified by the zero-flux condition $\nabla\rho \cdot \mathbf{n} = 0$. Both the ChelpG and QTAIM methods appear to be relatively insensitive to basis set errors [30, 43, 46], unlike the Mulliken population analysis.

The ChelpG atomic charges were calculated from the electronic density using the ChelpG routine of the Gaussian package, imposing the restriction that the ChelpG total cluster dipole moment reproduce the MP2/aug-cc-pvdz value calculated directly from the electronic density. For a discrete charge distribution obtained from the ChelpG optimization, the dipole moment of a molecule can be calculated in the standard way as a sum over the products of

TABLE II: The effect of the charge model on the calculated dipole moment of a water molecule in a water dimer by the ChelpG charges, in which one water molecule is treated at the MP2 level and the other one is represented by a charge model. The final entry is the result when both water molecules are treated at the MP2 level followed by ChelpG determination of the dipole of one of the waters.

| Charge Model | μ_{ChelpG} (Debyes) |
|--------------|-------------------------|
| TIP3P | 2.08 |
| TIP4P | 2.08 |
| AMOEBA | 2.09 |
| MP2 | 2.12 |

the effective atomic charges and the atomic locations relative to a reference point; the reference point does not affect the dipole for a neutral molecule. The ChelpG and QTAIM charge analyses below suggest, however, that there is a certain degree of charge transfer between the ion and neighboring water molecules. For example, on average, there is a charge transfer in the amount of roughly 0.03-0.05e in a $\text{Cl}^-/(\text{H}_2\text{O})_6$ cluster from the Cl^- ion to each coordinating water molecule. The dipole moment of a water molecule is not uniquely defined if the water molecule is not neutral. Since the amount of charge transfer to each water molecule is relatively small, we chose the water reference point to be the oxygen atom of the considered water molecule. To obtain an estimate of the dipole magnitude of the anion, the ChelpG fit was extended to include a point dipole on the anion; all other ChelpG charge fits were performed with a single charge on the chloride ion. The QTAIM net ion charges were computed with a code developed by Henkelman, Arnaldsson, and Jönsson [47].

We utilized the AMOEBA multipole and induced dipole model for waters beyond the first shell and implemented a localized effective charge distribution to mimic the field generated by those fixed and induced multipoles; discrete charges were distributed near the location of the point dipoles and quadrupoles so as to accurately mimic the electrostatic potential away from the multipoles. These charges were then used to generate an external potential in the Gaussian code. We tested this model against higher level *ab initio* calculations. Table II shows the effect of the charge model on the ChelpG calculated dipole moment of a water molecule in a water dimer, in which one water molecule is treated on the MP2 level and the other one is represented by a charge model. We found that all three water charge models (TIP3P, TIP4P, and AMOEBA) provide a reasonable field to reproduce the dipole moment calculated at the MP2 level. To be consistent with the molecular dynamics model, we chose the AMOEBA model for the external field.

III. COMPUTATIONAL RESULTS

A. Local hydration structure in AMOEBA simulations

The radial distribution functions (RDFs: $g(r)$) between the Cl^- ion and water molecules (O and H atoms) are shown in Figure 1 for chloride ion polarizabilities of 4 (default) and 2 \AA^3 . The effect of the anion polarizability on the first peaks of the Cl^- -H and Cl^- -O RDFs is small; the first minimum in the Cl^- -O RDF for the 2 \AA^3 polarizability case becomes slightly deeper, however, relative to the default polarizability value, likely due to a somewhat stronger attraction between the more-polarized ion and second-shell waters for the 4 \AA^3 polarizability case. The RDF for the Cl^- ion and oxygens of water shows a first peak at ~ 3.2 \AA , which agrees with the experimental Cl^- - H_2O bond length obtained by X-ray and neutron diffraction measurements [48, 49]. The first peak has a distribution range from 2.9 \AA to ~ 4.0 \AA . The RDF for the ion and hydrogens of water contains a nearest-neighbor peak near 2.3 \AA . The first minimum of the Cl^- -H RDF occurs around 3 \AA . The coordination number for Cl^- in H_2O obtained by integration of the Cl^- -H pair distribution function up to the first minimum is 5.9 for the default chloride ion polarizability and 6.2 for the reduced polarizability case. The instantaneous coordination number is defined as the number of hydrogens within 3 \AA (the first minimum in the Cl-H pair correlation function) with an O-H...Cl angle greater than 130 $^\circ$ (a commonly used lower limit in hydrogen bond analysis). Figure 2 displays the log of the coordination number as a function of n and shows that the instantaneous coordination number fluctuates in the range 2 to 9 with a maximum probability at 6. The average coordination number is 5.5 for the 4 \AA^3 polarizability case, slightly less than that obtained by integration of the RDFs due to the angular hydrogen-bonding restriction. Reduced anion polarizability shifts the coordination number distribution to slightly larger coordination numbers, with an average value of 5.8. These structural results are qualitatively similar to Car-Parrinello molecular dynamics density functional theory (CPMD-DFT) simulations of the chloride and bromide ions in water [16, 50]. We note that coordination number distributions, along with occupancy numbers for waters in the same observation volume, can yield free energies differences between the various coordination states [51].

Figure 3 shows that, for the default chloride ion polarizability simulation, the distance between the center of mass

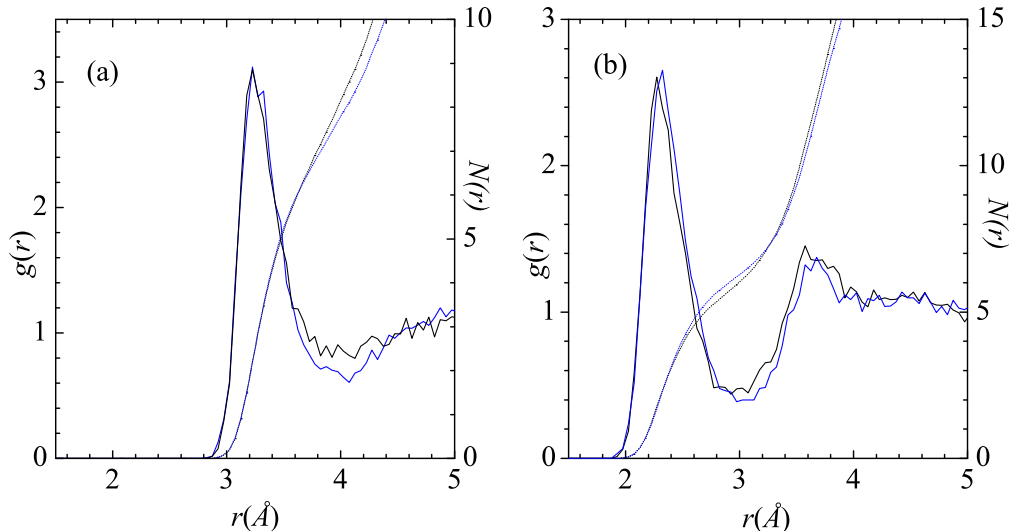


FIG. 1: Radial distribution functions $g(r)$ and integrated values $N(r)$ from the AMOEBA simulations: (a) chloride/(water oxygen) and (b) chloride/(water hydrogen). The black curves are for the default chloride ion polarizability simulation, while the blue curves are for the reduced ion polarizability simulation.

of first shell waters and the Cl^- ion, R_{cage} , fluctuates in the range 0.1 to 2.5 Å with a peak around 1 Å. Comparison of the distribution with that for the Na^+ ion suggests an increased anisotropy of the solvation shell around the chloride ion. That anisotropy is reduced when the chloride ion polarizability is reduced by a factor of two, consistent with our previous simulations [20]. Significant anisotropy relative to the Na^+ ion distribution is still apparent, however, even at the lower polarizability. Since the computed probability distribution involves a radial coordinate, we also plot the distribution divided by $4\pi R_{\text{cage}}^2$; increased solvation anisotropy then shows up as a significantly reduced probability at small radii relative to the sodium case. Figure 4 displays three snapshots of the ion and the first-shell waters in typical configurations from the default ion polarizability simulations to illustrate the anisotropic solvation. We have observed some typical configurations of the inner solvation shell, such as 4, 4+1, or 4+2. A careful investigation of the trajectories suggests that the first solvation shell of the chloride ion contains many low energy conformers at room temperature; it is thus difficult to identify a unique hydration structure. All these conformers exhibit anisotropic structures, however; similar results have been found in surface-like states reported for $\text{Cl}^-(\text{H}_2\text{O})_n$ clusters [52] and Br^- ions in water [50]. Wick and Xantheas [53] have suggested that the extinction of the small cavity on the water-depleted side of the ion may create a driving force for anion interfacial activity.

B. Ion and water dipole moments and charge transfer

As discussed in a wide range of studies [54, 55, 56, 57, 58, 59, 60], anion segregation to the water liquid/vapor interface likely results from a subtle balance of anion-water and water-water interactions. In the following, we study the dipole moments of the ion and the water molecules in the bulk first solvation shell and charge transfer effects, utilizing high level quantum chemistry methods. Also we investigate how the polarization of water molecules in the first solvation shell changes in the presence of the ion, nearby waters in the first shell, and the surrounding water molecules beyond the first shell. The goal is to provide an accurate physical description of the ion-water and water-water interactions in the first solvation shell where the classical potential may not suffice for quantitatively answering polarization questions. All the calculations are performed at the MP2/aug-cc-pvdz level based on the clusters extracted from the trajectories generated by the simulation with the AMOEBA force field. The effect of the solvating environment (second and further solvation shells) is handled with the charge model discussed in Section II.

Molecular dipole moments are quantities which characterize the charge distribution in molecules. Charge redistribution or electronic polarization due to interaction of molecules with the external environment is directly reflected by the change in the magnitude of the dipole moments in the various systems we study. Higher-order polarization

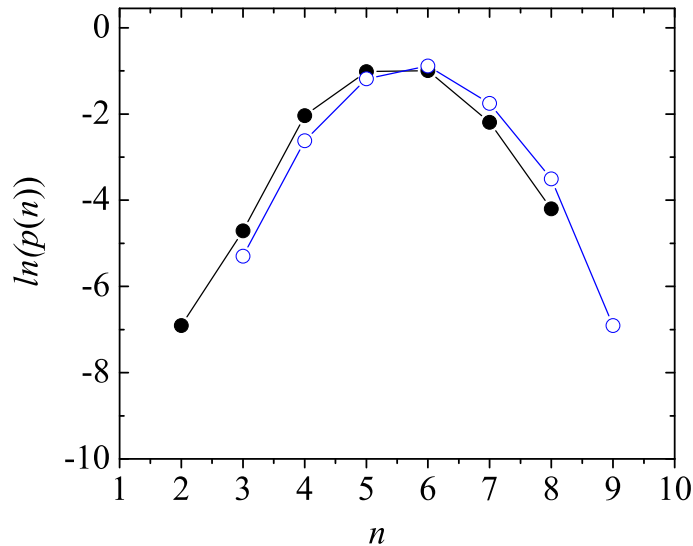


FIG. 2: The log of the distribution of the coordination number n of Cl^- (aq) from the AMOEBA simulation. The curve shown in black is for the default ion polarizability simulation, while the blue curve is for the reduced ion polarizability simulation.

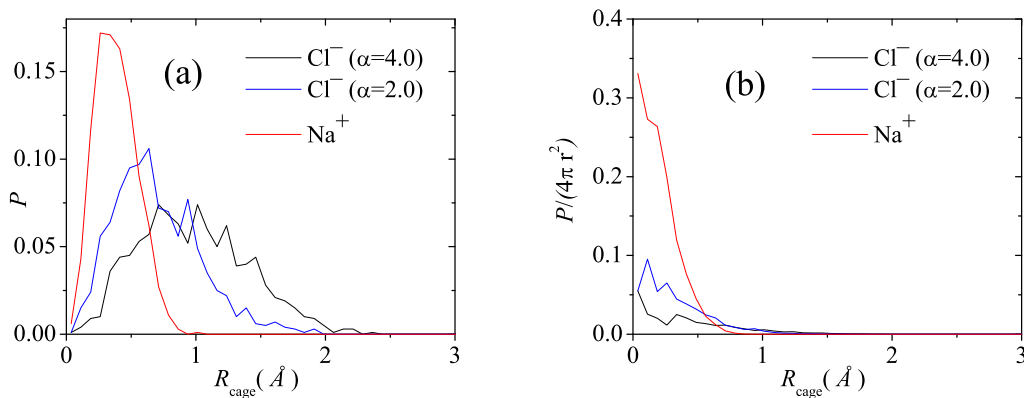


FIG. 3: (a) The distributions of R_{cage} , the distance between the center of mass of the first solvation shell water O atoms and the Na^+ and Cl^- ions, from the AMOEBA simulations. (b) The distributions divided by $4\pi R_{\text{cage}}^2$.

effects can be expected to contribute to the interactions, but analysis of the dipoles can give an initial view of molecular charge redistributions. We utilize the ChelpG charges and dipoles to investigate the dipole moments of water molecules and ions averaged over configurations equally spaced in time by 1 ps. The configurations are taken from the trajectories of the AMOEBA simulation. The quantum results are compared to the dipole moments calculated from the AMOEBA model.

The calculated anion and first-shell water dipole distributions are shown in Figure 5. We first present the results for the chloride ion charge distribution. As discussed above, the ChelpG fitting was augmented by inclusion of a point dipole on the chloride ion to obtain an estimate of the dipole moment from the MP2 calculations. For the default anion polarizability AMOEBA simulation, the average dipole moment magnitude of the chloride ion from the MP2-ChelpG method is 0.6 D (standard deviation of 0.2 D); this differs significantly from the AMOEBA model result of 1.6 D (standard deviation of 0.5 D). For the reduced anion polarizability AMOEBA simulation, the average dipole moment magnitudes of the chloride ion from the MP2-ChelpG and AMOEBA methods are 0.5 D (standard

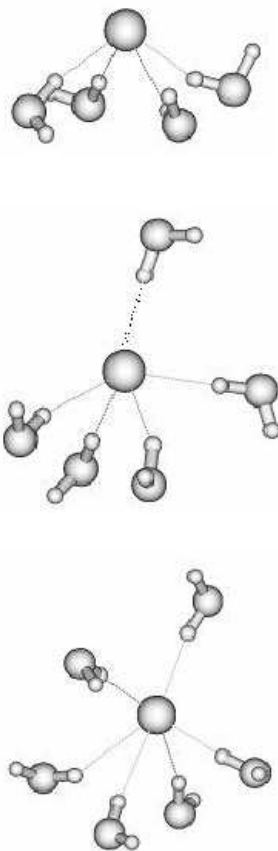


FIG. 4: Three snapshots of typical configurations of the $\text{Cl}^-/\text{H}_2\text{O}$ first hydration shell from a simulation with the AMOEBA force field (default ion polarizability).

deviation of 0.2 D) and 1.0 D (standard deviation of 0.4 D), respectively. Thus the quantum result decreases slightly with reduced anion polarizability, presumably due to a less anisotropic hydration environment, while the AMOEBA result decreases substantially. Our MP2 calculations are consistent with recent extensive AIMD-DFT studies of the chloride ion [17, 61] and the bromide ion [50] in water, where average dipole moments of 0.8 D for the chloride ion and 0.9 D for the bromide ion were observed. The AIMD simulations utilized a Wannier decomposition to estimate the dipole moments; that procedure places full electron charges on individual atoms. As will be discussed below, we observe a charge transfer of 0.2e from the chloride ion to the nearby waters. When that charge transfer effect is taken into account, our results are entirely consistent with the estimate from Ref. [17] and may provide a more accurate estimate of the average dipole magnitudes.

On the other hand, Wick and Xantheas [53] used the polarizable Dang-Chang model to study a chloride ion in water and found an average ion dipole moment of about 1.3 - 1.5 D, which is similar to our AMOEBA calculations (see also Ref. [20]). Thus, the Dang-Chang and AMOEBA models appear to significantly overestimate the anion dipoles. This discrepancy may arise from the fact that these classical polarizable models contain no or limited damping of the nearby electrostatic interactions for the self-consistent polarization calculation [61]. In addition, these classical models do not account for charge transfer; force fields to handle charge transfer are under active development [62, 63]. Wick [60] has recently shown that increased local damping of the charged interactions during the polarization self-consistency step, leading to smaller anion dipoles, reduces the surface affinity of anions at the water liquid-vapor interface.

In the AMOEBA model, point polarizable dipoles (in addition to the fixed multipoles) are located on the ion and on each atom within the water molecule. At short distances there may be diffuse electron distributions, significant electron density overlap, and possible charge transfer between the ion and the water molecules. Thus it is a challenge for the multipole-based models to reproduce these complex chemical effects, and the effectiveness of the models should be tested against electronic structure methods. Work along these lines has been initiated by Masia and coworkers [17, 61, 64]. To further explore these issues, we next examine possible charge transfer effects between the anions and their neighboring hydration shell.

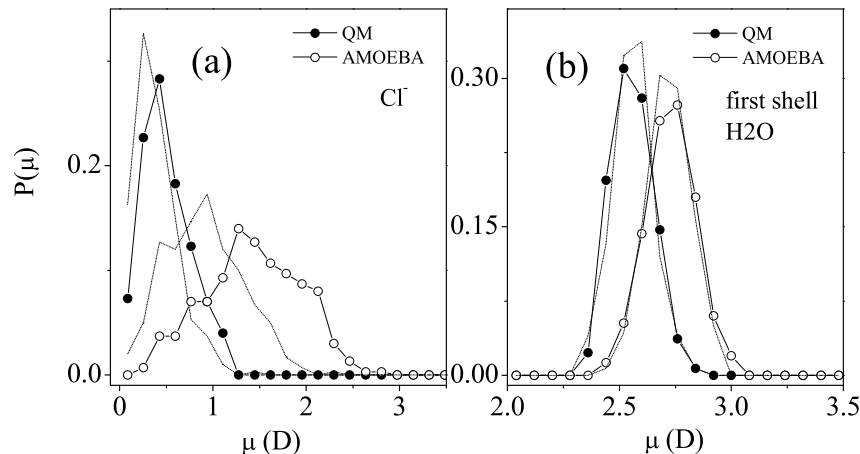


FIG. 5: The distribution of the magnitude of (a) the anion and (b) first-shell water molecule dipole moments (μ). In (a) the solid and filled circles represent the distribution of μ for the Cl^- ion calculated at the MP2-ChelpG level and the classical AMOEBA model level, respectively (default chloride ion polarizability case). The curves without symbols are for the reduced chloride ion polarizability simulations. In (b) the solid and filled circles represent the distribution of μ for water molecules in the first solvation shell of the anion at the MP2-ChelpG level and at the classical AMOEBA model level, respectively (default chloride ion polarizability case). The curves without symbols are for the reduced chloride ion polarizability simulations.

Charge transfer has been observed in the study of anion-water clusters and anions in bulk water [65, 66, 67, 68, 69, 70, 71]. To study these effects with our QM/MM model, we calculated the charge on the chloride ion using both the ChelpG and the QTAIM methods. Both approaches have been shown to be relatively accurate methods for the calculation of the amount of intermolecular electron transfer [30]. The calculated distribution of anion charges is shown in Figure 6. For the default chloride ion polarizability AMOEBA simulation, the average charge of the chloride ion is -0.7 from the ChelpG method and -0.8 from the QTAIM analysis. While these effective charge values are relatively close to each other, it can be seen from the figure that the distributions differ appreciably; this is not surprising since the charges are determined by quite different strategies. Due to its more rigorous physical underpinning, we view the QTAIM charge calculations as a more accurate indication of the net charge on the anions relative to the ChelpG results. The calculations suggest charge transfer in the amount of $\sim 0.2e$ from the chloride ion to the nearby hydration shell. Modeling the chloride ion with a polarizability of 2 \AA^3 resulted in only slight changes in the distributions of ion charge states (Figure 6). The observation of significant charge transfer is consistent with the previous CPMD study by Dal Peraro and co-workers [66] and electronic structure calculations on anions in water [71]. Rashin *et al.* [72] applied a different charge partitioning scheme and concluded that charge transfer in ion-water clusters is not as significant as the results discussed above.

In order to analyze the differences between the ChelpG and QTAIM estimates of charge transfer observed in Figure 6, configurations were extracted from the AMOEBA simulations for clusters with $N = 1 - 4$ waters. These random configurations were then optimized at the MP2 level to generate unique structures. Table III lists the computed charges from the ChelpG method (one charge only on the chloride ion), ChelpG with an added point dipole on the chloride ion, and the QTAIM method. The chloride ion dipoles estimated by the ChelpG calculations are given in the last column. It is clear from these data that the addition of the dipole in the ChelpG ESP fitting reduces the estimated charge transfer relative to the fit with only a single charge placed on the ion. Also, for the $N = 3$ and $N = 4$ cases, the ChelpG estimate including the dipole is close to the QTAIM value. In principle, higher-order multipoles could also be included in the fitting procedure, but we don't follow that direction here. Thus it would appear that the ChelpG distribution presented in Figure 6 (with only a single charge included on the ion during the ESP fit) would likely shift closer to the QTAIM distribution with inclusion of a point dipole (or higher multipoles) in the fitting. Figure 7 displays an electron density contour plot for the $N = 1$ case in the plane determined by the chloride ion and the water hydrogen and oxygen. Also displayed is the electron density difference contour plot for the same $\text{Cl}^-/\text{H}_2\text{O}$ complex; the polarization of the chloride ion is apparent from a withdrawal of electron density from the opposite side of the ion from the water molecule and buildup in the direction of the hydrogen bond. The re-distribution of charge

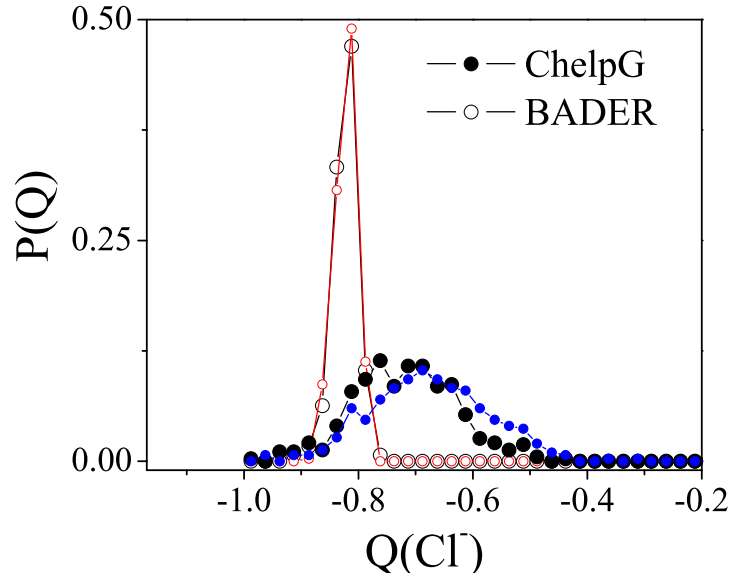


FIG. 6: Shown are the distributions of charges on the Cl^- ion calculated using the ChelpG scheme and the QTAIM analysis. The curves with filled circles are from the ChelpG analysis; the black curve is for the default chloride ion polarizability simulation, while the blue curve is for the reduced polarizability case. The curves labeled with open circles are from the QTAIM analysis; the black curve is for the default chloride ion polarizability simulation, while the red curve is for the reduced polarizability case. The ion/(first-shell water) cluster QM/MM calculations included electrostatic interactions with more distant waters via the charge model described in Section II.

TABLE III: Charges on the chloride ion estimated by the ChelpG and QTAIM methods. Columns 2-4 display the results for the ChelpG method with a single charge on the chloride ion, the ChelpG method with an added dipole on the chloride ion, and the QTAIM method, respectively. The final column is the estimated dipole moment on the chloride ion obtained from the calculations in column 3.

| N | ChelpG(Q) | ChelpG-d(Q) | QTAIM(Q) | ChelpG(μ -D) |
|-----|---------------|-----------------|--------------|-------------------|
| 1 | -0.938 | -0.977 | -0.918 | 0.24 |
| 2 | -0.873 | -0.944 | -0.892 | 0.36 |
| 3 | -0.830 | -0.880 | -0.874 | 0.27 |
| 4 | -0.805 | -0.830 | -0.847 | 0.10 |

on the water molecule is interesting in that there appears to be some depletion in the region of the hydrogen bond to the ion, and a buildup on the other side of the water molecule. These charge redistributions may be related to recent measurements of the oxygen K-edge X-ray absorption spectrum (XAS) of aqueous sodium halide solutions, which suggest perturbations of unoccupied water orbitals due to interactions with anions [73]. The electron density and difference contour plots indicate that the overall charge distribution is complicated with significant electron density overlap and rearrangement; this suggests a multipole expansion to represent the ESP due to the ion may be questionable. On the other hand the QTAIM estimate of the ion charge is based on a direct physical criterion derived from the electron density. We note that the QTAIM estimate of the charge transfer is roughly additive with increasing numbers of waters (after the first water), indicating each additional hydrogen bond makes a similar contribution. The locations of the hydrogen bonds fluctuate widely, however, during thermal sampling, leading to complex and varying charge distributions for the chloride ion.

Next we discuss the results for the dipole distributions in the first-shell water molecules. The average value of the dipole moment of the water molecules in the first solvation shell is close to, but slightly less than, the bulk AMOEBA water value (2.78 D) for both the MP2-ChelpG and the AMOEBA calculations; the MP2-ChelpG estimate is 2.67 D while the AMOEBA model prediction is 2.72 D. Figure 5 presents the distributions of instantaneous first-shell water dipole magnitudes; neither the MP2-ChelpG nor the AMOEBA distributions change appreciably with reduced chloride ion polarizability in the AMOEBA simulations. Raugai and Klein’s [50] CPMD study of the bromide ion

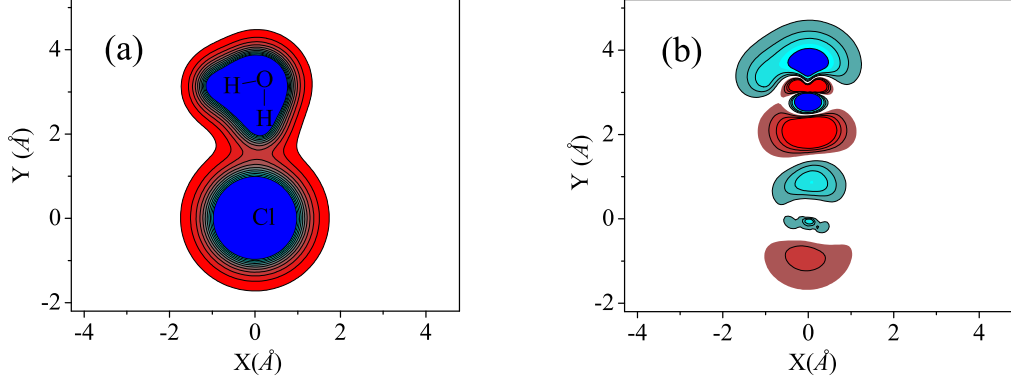


FIG. 7: (a) Contour plot of the total electron density for the $\text{Cl}^-/(\text{H}_2\text{O})$ dimer. The chosen plane contains the hydrogen bond between the ion and the water hydrogens. (b) Contour plot of the electron density difference between the $\text{Cl}^-/\text{H}_2\text{O}$ complex and the separated ion and water molecule. The configuration and plane are the same as in (a). Red indicates reduced electron density, and shades of blue imply increased electron density.

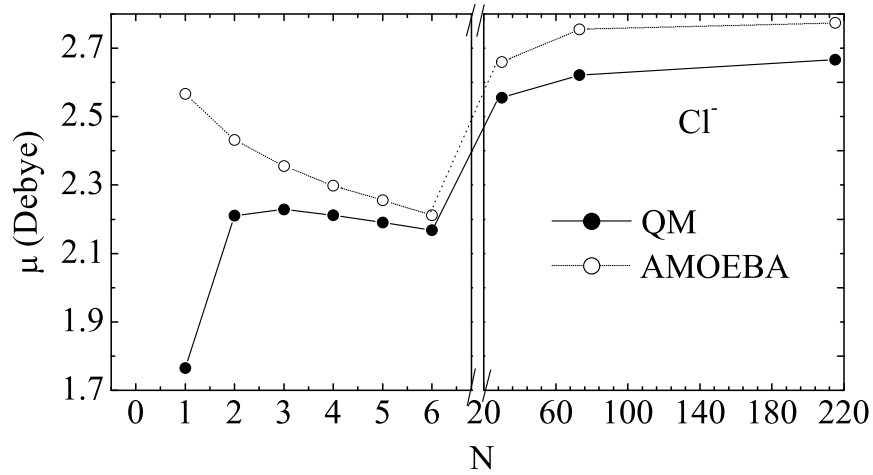


FIG. 8: The magnitude of the average dipole moment μ of water molecules neighboring a Cl^- ion as a function of increasing cluster size N . On the left, the system modeled included the ion and the given number of water molecules. On the right, 6 waters were treated quantum mechanically in the first shell, and the rest of the waters in the QM/MM cluster were represented with AMOEBA charges distributed as described in Section II.

in water also suggested the water molecules in the first shell possess dipole moments close to those of bulk water molecules. Recent extensive AIMD simulations have shown slightly suppressed water dipoles in the first solvation shell for the larger halides [17] and the K^+ ion [18], in agreement with our AMOEBA and MP2 results.

To further investigate which interactions are most responsible for the polarization of water molecules in the first shell and the interplay of ion-water and water-water interactions, we studied the magnitude of the average dipole moment of the water molecules neighboring the chloride ion as a function of increasing cluster size N , as shown in Figure 8. Only the default chloride ion polarizability case was considered in examining the size dependence, since the anion polarizability had a relatively small effect on the water dipole distributions. The first 6 water molecules are treated at the MP2 level, while more distant waters are handled with the effective charge model obtained from the AMOEBA simulation.

As we increase the ion-water cluster size ($N = 1-6$), we find that the average dipole moment of the water molecules in the first hydration shell of the ion (at the QM/MM level) first increases to a value around 2.2 D and then stays roughly constant (decreasing slightly with increasing N). We note that, in our calculations, the numbering is such that the second and successive water molecules are chosen as the nearest water to the preceding water oxygen. This choice was made in order to explore the effects of nearby water-water interactions. The average distance between the two water molecules, measured by the distance between the two O atoms, is around 3.5 Å. The addition of a second water molecule significantly increases the polarization of the first water molecule, even though there is no direct hydrogen bonding between the two water molecules. The appreciable deviation between the quantum and AMOEBA results for the $N = 1$ case may be tied to the larger charge transfer to the closest water discussed above. Further addition of water molecules in the first hydration shell doesn't substantially affect the polarization of water molecules on average. Previous reports examining polarization for hydration shell water molecules of anions displayed a different N dependence for the water dipoles [74]. This is likely because of the different $\text{Cl}^-/(\text{H}_2\text{O})_n$ cluster structures investigated. We utilize the instantaneous cluster structures extracted from the molecular dynamics simulation, while Ref. [74] used optimized gas phase cluster structures. Comparing our MP2 calculations with the AMOEBA calculations, we find the AMOEBA model slightly overestimates the dipole moments of the water molecules in the first shell for $N \geq 2$, with better agreement as N increases.

Finally, we study the effect of the second solvation shell and further shell water molecules on the polarization of the first shell water molecules. We find that the addition of the second solvation shell (represented as sets of charges so as to reproduce the AMOEBA multipole potential) with formation of direct hydrogen bonding to those external waters increases the average dipole moment of the first shell water molecules further by about 20%. Third and further solvation shells don't appear to have a large impact on the polarization of the first shell water molecules. As discussed above, upon full hydration the average dipole magnitude is 2.67 D for the inner-shell water molecules, which is slightly smaller than the AMOEBA value of 2.72 D and close to the AMOEBA value for bulk water (2.78 D). We note that the water dipole values presented here are somewhat below those observed in AIMD-DFT simulations [16, 17, 50]; an experimental estimate for bulk water is 2.9 D [75]. The results support the picture suggested by Rauei and Klein [50], Krekeler and Delle Site [76], and Guàrdia, Skarmoutsos, and Masia [17] that the anion scarcely influences the polarization of the water molecules in the first solvation shell; in fact the inner-shell waters appear to have average dipole magnitudes slightly reduced from the bulk value. We observe that the first-shell water-water interactions (modified by interactions with the ion) and the H-bonding environment from the second solvating shell are the major factors that determine the polarization of the first shell water molecules. This result supports the idea suggested by Devereux and Popelier that the local H-bonding environment of a water molecule determines its charge distribution and electronic properties [77].

IV. CONCLUSIONS AND DISCUSSION

This paper has examined the local structure and polarization involved in chloride ion hydration with a QM/MM treatment. Classical polarizable force field molecular dynamics simulations were performed with the AMOEBA model. Clusters were extracted from the simulations for further analysis with quantum chemical methods at the MP2-level of electronic structure theory. The clusters treated quantum mechanically involved the ion and the nearest waters in the first solvation shell. The inner-shell clusters interacted with more distant waters modeled with AMOEBA charge distributions. In particular, we examined the average dipole magnitudes for the chloride ion and the nearby waters, and charge transfer from the anion to the waters. The role of interactions with waters outside the first shell was explored by successively increasing the size of the QM/MM clusters.

In the classical polarizable AMOEBA simulations, anisotropic solvation structures were observed around the chloride ion, consistent with other classical models [53] and AIMD simulations [50]. The anisotropy decreases with decreasing chloride ion polarizability, but is still significant with the polarizability reduced by a factor of 2. The solvation anisotropy is clear from visual inspection of representative configurations, and from examination of the location of the center-of-mass of the inner-shell waters relative to the chloride ion location. The most probable coordination number observed in the AMOEBA simulations is 6 based on a standard hydrogen-bonding criterion.

The first-shell water molecule dipoles computed quantum mechanically (in the external field of surrounding waters) are slightly reduced relative to the AMOEBA model, and both exhibit slightly reduced values compared with bulk AMOEBA water. This result is somewhat surprising, but is consistent with recent AIMD-DFT simulations [17, 18]. Reducing the chloride ion polarizability in the AMOEBA simulations had little effect on the first-shell water dipoles. We find that water-water interactions within the inner shell and further interactions with more distant waters are all crucial in determining the polarization state of the inner-shell waters. In fact, the water-water interactions appear to dominate over the ion-water interactions in the polarization [76].

The average chloride ion dipole moments computed quantum mechanically are significantly lower than those ob-

served in the AMOEBA simulations, however. Such behavior has also been found in several AIMD simulations [16, 17, 50], and it thus appears that the AMOEBA model, even with Thole-type damping incorporated for the nearby electrostatic interactions, is over-polarizing the chloride ion. Since we showed in another study [20] that the polarization is linked to solvation anisotropy, this finding raises the issue that some of the previous classical polarizable models may be consistently over-estimating solvation anisotropy. The quantum mechanical ion dipoles were reduced slightly when the configurations were sampled with the lower chloride polarizability, presumably due to the lower anisotropy in the first-shell waters. The issue of designing damping functions that properly represent the ion dipoles in classical simulations has been addressed by Masia [61].

In addition, we observe significant charge transfer from the chloride ion to the nearby waters (0.2e from the QTAIM method). Charge transfer has been implicated in a wide range of biophysical solvation problems [78] and has been previously observed in DFT simulations [66] and quantum chemical studies [71, 79, 80]. It is possible that the over-polarized ions observed in the AMOEBA model somehow mimic this charge transfer effect, but further work is necessary to quantify the relation of the classical models to the more realistic quantum calculations. Since most models used to study the surface affinity of anions to the water liquid-vapor interface have employed no electrostatic damping, or limited versions as in the AMOEBA model, these issues should be revisited in modeling the specific ion effects. A recent study has confirmed that reduced ion polarization in turn reduces anion surface affinity [60].

We have chosen a QM/MM approach with an MP2-level treatment of the inner shell for several reasons. First, this level of theory should generate relatively accurate charge distributions for analysis of local polarization around the ions [81]. Second, MP2 calculations include dispersion interactions at a decent level of accuracy, and we believe this is important for accurately modeling ion-water and water-water interactions [82]. Third, we plan to couple this QM/MM approach to computations of solvation free energies via quasi-chemical theory [19, 20, 83]. In the quasi-chemical approach, the solvation free energy is exactly partitioned into inner-shell, outer-shell packing, and outer-shell long-range contributions. The conditioning inherent in this partitioning allows for a mean-field treatment of the long-range contribution. We have observed in another study [20] that relatively small conditioning radii already lead to Gaussian behavior in the long-ranged contribution. With such small conditioning radii, most of the hydration free energy is contained in the long-ranged part, and that term can then be examined for the various contributions to ion specificity. We plan to compute the solvation free energies in our MP2-level QM/MM model, and further explore the various contributions to the free energy (charge-charge, induction, dispersion) via an SAPT energy division [84, 85]. Even though there have been multiple indications that polarization is crucial for anion solvation, it may be possible that dispersion interactions will play a more important role in ion specificity than predicted by classical polarizable models [7].

Computing effective water and ion charges and dipoles can provide helpful insights into the local solvation structure. These charges and multipoles could then serve as input for the development of more refined molecular dynamics force fields. An alternative suggestion, however, is that the ion solvation environment involves complicated and diffuse charge distributions best represented with electronic structure methods. The quasi-chemical treatment of solvation thermodynamics provides a natural statistical mechanical framework for representing the first solvation shell at an accurate quantum mechanical level, with a lower-level representation of more distant waters [86, 87, 88].

V. ACKNOWLEDGMENTS

We gratefully acknowledge the support of NSF grant CHE-0709560. We acknowledge the Ohio Supercomputer Center for a grant of computing time. We thank Marco Masia for comments on the paper.

-
- [1] W. D. Stein, *Channels, Carriers, and Pumps* (Academic Press Inc, New York, 1990).
 - [2] B. Hille, *Ion Channels of Excitable Membranes* (Sinauer Associates Inc, Sunderland, 2001), 3rd ed.
 - [3] L. J. DeFelice, *Trends Neurosci.* **27**, 352 (2004).
 - [4] A. Accardi and C. Miller, *Nature* **427**, 803 (2004).
 - [5] J. Yin, Z. Kuang, U. Mahankali, and T. Beck, *Proteins: Struct., Func., and Bioinform.* **57**, 414 (2004).
 - [6] Z. F. Kuang, U. Mahankali, and T. L. Beck, *Proteins: Struct., Func., and Bioinform.* **68**, 26 (2007).
 - [7] W. Kunz, P. Lo Nostro, and B. W. Ninham, *Curr. Opin. Colloid Interface Sci.* **9**, 1 (2004).
 - [8] H. I. Petrache, T. Zemb, L. Belloni, and V. Parsegian, *Proc. Natl. Acad. Sci. USA* **103**, 7982 (2006).
 - [9] Y. J. Zhang and P. S. Cremer, *Curr. Op. Chem. Biol.* **10**, 658 (2006).
 - [10] B. Ninham and M. Bostrom, *Cell. Molec. Biol.* **51**, 803 (2005).
 - [11] R. H. Wood, E. M. Yezdimer, S. Sakane, J. A. Barriocanal, and D. J. Doren, *J. Chem. Phys.* **110**, 1329 (1999).
 - [12] S. Sakane, E. M. Yezdimer, W. B. Liu, J. A. Barriocanal, D. J. Doren, and R. H. Wood, *J. Chem. Phys.* **113**, 2583 (2000).

- [13] W. Liu, D. J. Doren, and R. H. Wood, *J. Chem. Phys.* **118**, 2837 (2003).
- [14] S. Sakane, W. B. Liu, D. J. Doren, E. L. Shock, and R. H. Wood, *Geochim. Cosmochim. Acta* **65**, 4067 (2001).
- [15] K. Laasonen and M. L. Klein, *Molec. Phys.* **88**, 135 (1996).
- [16] J. M. Heuft and E. J. Meijer, *J. Chem. Phys.* **119**, 11788 (2003).
- [17] E. Guárdia, I. Skarmoutsos, and M. Masia, *J. Chem. Theory Comput.* **5**, 1449 (2009).
- [18] T. W. Whitfield, S. Varma, E. Harder, G. Lamoureux, S. B. Rempe, and B. Roux, *J. Chem. Theory Comput.* **3**, 2068 (2007).
- [19] D. M. Rogers and T. L. Beck, *J. Chem. Phys.* **129**, 134505 (2008).
- [20] D. M. Rogers and T. L. Beck (2009), submitted.
- [21] P. Y. Ren and J. W. Ponder, *J. Phys. Chem. B* **108**, 13427 (2004).
- [22] P. Y. Ren and J. W. Ponder, *J. Phys. Chem. B* **107**, 5933 (2003).
- [23] P. Y. Ren and J. W. Ponder, *J. Comput. Chem.* **23**, 1497 (2002).
- [24] D. Case, T. Darden, T. I. Cheatham, C. Simmerling, J. Wang, R. Duke, R. Luo, M. Crowley, R. C. Walker, W. Zhang, et al., *AMBER 10* (University of California, San Francisco, 2008).
- [25] A. Grossfield, P. Y. Ren, and J. W. Ponder, *J. Am. Chem. Soc.* **125**, 15671 (2003).
- [26] U. Essmann, L. Perera, M. L. Berkowitz, T. Darden, H. Lee, and L. G. Pedersen, *J. Chem. Phys.* **103**, 8577 (1995).
- [27] M. J. Frisch, G. W. Trucks, H. B. Schlegel, G. E. Scuseria, M. A. Robb, J. R. Cheeseman, J. J. A. Montgomery, T. Vreven, K. N. Kudin, J. C. Burant, et al., *Gaussian 03, Revision D.01*, Gaussian, Inc., Wallingford, CT, 2004.
- [28] T. H. Dunning, *J. Chem. Phys.* **90**, 1007 (1989).
- [29] A. Volkov, H. F. King, and P. Coppens, *J. Chem. Theor. Comput.* **2**, 81 (2006).
- [30] B. Szeftczyk, W. A. Sokalski, and J. Leszczynski, *J. Chem. Phys.* **117**, 6952 (2002).
- [31] W. Benedict, N. Gailar, and E. Plyler, *J. Chem. Phys.* **24**, 1139 (1956).
- [32] F. Lovas, *J. Phys. Chem., Ref. Data* **7**, 1445 (1978).
- [33] C. M. Breneman and K. B. Wiberg, *J. Comput. Chem.* **11**, 361 (1990).
- [34] P. I. Nagy, G. Alagona, and C. Ghio, *J. Chem. Theor. Comput.* **3**, 1249 (2007).
- [35] E. Mayaan, A. Moser, A. D. MacKerell, and D. M. York, *J. Comput. Chem.* **28**, 495 (2007).
- [36] F. Dommert, J. Schmidt, C. Krekeler, Y. Y. Zhao, R. Berger, L. Delle-Site, and C. Holm, *J. Molec. Liqs.* (2009), in press.
- [37] G. Kamath, G. Georgiev, and J. J. Potoff, *J. Phys. Chem. B* **109**, 19463 (2005).
- [38] A. R. Katritzky, N. G. Akhmedov, J. Doskocz, P. P. Mohapatra, C. D. Hall, and A. Guven, *Mag. Res. Chem.* **45**, 532 (2007).
- [39] R. F. W. Bader, *Atoms in molecules: a quantum theory* (Clarendon Press, Oxford, 1990).
- [40] R. F. W. Bader, A. Larouche, C. Gatti, M. T. Carroll, P. J. Macdougall, and K. B. Wiberg, *J. Chem. Phys.* **87**, 1142 (1987).
- [41] G. S. Maciel and E. Garcia, *Chem. Phys. Lett.* **409**, 29 (2005).
- [42] T. C. F. Gomes, J. V. da Silva, L. N. Vidal, P. A. M. Vazquez, and R. E. Bruns, *Theor. Chem. Acct.* **121**, 173 (2008).
- [43] F. Martin and H. Zipse, *J. Comput. Chem.* **26**, 97 (2004).
- [44] M. Masamura, *Struct. Chem.* **11**, 41 (2000).
- [45] P. E. Blöchl, *J. Chem. Phys.* **103**, 7422 (1995).
- [46] S. Tsuzuki, T. Uchimaru, K. Tanabe, and A. Yliniemela, *J. Molec. Struct. (Theochem)* **365**, 81 (1996).
- [47] G. Henkelman, A. Arnaldsson, and H. Jonsson, *Comput. Mater. Sci.* **36**, 354 (2006), available at <http://theory.cm.utexas.edu/bader/>.
- [48] G. Palinkas, T. Radnai, and F. Hajdu, *Zeit. Naturforsch. Sec. A* **35**, 107 (1980).
- [49] N. Ohtomo and K. Arakawa, *Bull. Chem. Soc. Jap.* **53**, 1789 (1980).
- [50] S. Raugei and M. L. Klein, *J. Chem. Phys.* **116**, 196 (2002).
- [51] D. Asthagiri, P. D. Dixit, S. Merchant, M. E. Paulaitis, L. R. Pratt, S. B. Rempe, and S. Varma (2009), preprint.
- [52] D. J. Tobias, P. Jungwirth, and M. Parrinello, *J. Chem. Phys.* **114**, 7036 (2001).
- [53] C. A. Wick and S. S. Xantheas, *J. Phys. Chem. B* **113**, 4141 (2009).
- [54] M. A. Carignano, G. Karlstrom, and P. Linse, *J. Phys. Chem. B* **101**, 1142 (1997).
- [55] P. Jungwirth and D. J. Tobias, *Chem. Rev.* **106**, 1259 (2006).
- [56] M. Mucha, T. Frigato, L. M. Levering, H. C. Allen, D. J. Tobias, L. X. Dang, and P. Jungwirth, *J. Phys. Chem. B* **109**, 7617 (2005).
- [57] T.-M. Chang and L. X. Dang, *Chem. Rev.* **106**, 1305 (2006).
- [58] L. Perera and M. L. Berkowitz, *J. Chem. Phys.* **96**, 8288 (1992).
- [59] D. Hagberg, S. Brdarski, and G. Karlstrom, *J. Phys. Chem. B* **109**, 4111 (2005).
- [60] C. D. Wick, *J. Chem. Phys.* **131**, 084715 (2009).
- [61] M. Masia, *J. Chem. Phys.* **128**, 184107 (2008).
- [62] G. A. Kaminski, H. A. Stern, B. J. Berne, and R. A. Friesner, *J. Phys. Chem. A* **108**, 621 (2004).
- [63] J. H. Chen and T. J. Martinez, *Chem. Phys. Lett.* **438**, 315 (2007).
- [64] M. Masia, M. Probst, and R. Rey, *Chem. Phys. Lett.* **420**, 267 (2006).
- [65] J. E. Combariza, N. R. Kestner, and J. Jortner, *J. Chem. Phys.* **100**, 2851 (1994).
- [66] M. Dal Peraro, S. Raugei, P. Carloni, and M. L. Klein, *ChemPhysChem* **6**, 1715 (2005).
- [67] D. Bucher, S. Raugei, L. Guidoni, M. Dal Peraro, U. Rothlisberger, P. Carloni, and M. L. Klein, *Biophys. Chem.* **124**, 292 (2006).
- [68] W. H. Robertson, M. A. Johnson, E. M. Myshakin, and K. D. Jordan, *J. Phys. Chem. A* **106**, 10010 (2002).

- [69] W. H. Robertson and M. A. Johnson, *Annu. Rev. Phys. Chem.* **54**, 173 (2003).
- [70] W. Thompson and J. Hynes, *J. Am. Chem. Soc.* **122**, 6278 (2000).
- [71] A. V. Marenich, R. M. Olson, A. C. Chamberlin, C. J. Cramer, and D. G. Truhlar, *J. Chem. Theory Comput.* **3**, 2055 (2007).
- [72] A. A. Rashin, I. A. Topol, G. J. Tawa, and S. K. Burt, *Chem. Phys. Lett.* **335**, 327 (2001).
- [73] C. D. Cappa, J. D. Smith, K. R. Wilson, B. M. Messer, M. K. Gilles, R. C. Cohen, and R. J. Saykally, *J. Phys. Chem. B* **109**, 7046 (2005).
- [74] C. Krekeler, B. Hess, and L. Delle Site, *J. Chem. Phys.* **125**, 054305 (2006).
- [75] Y. S. Badyal, M.-L. Saboungi, D. L. Price, S. D. Shastri, D. R. Haeffner, and A. K. Soper, *J. Chem. Phys.* **112**, 9206 (2000).
- [76] C. Krekeler and L. Delle Site, *J. Phys.-Cond. Matt.* **19**, 192101 (2007).
- [77] M. Devereux and P. L. A. Popelier, *J. Phys. Chem. A* **111**, 1536 (2007).
- [78] K. D. Collins, G. W. Neilson, and J. E. Enderby, *Biophys. Chem.* **128**, 95 (2007).
- [79] W. H. Thompson and J. T. Hynes, *J. Am. Chem. Soc.* **122**, 6278 (2000).
- [80] S. G. Ramesh, S. Re, and J. T. Hynes, *J. Phys. Chem. A* **112**, 3391 (2008).
- [81] J. Kim, H. M. Lee, S. B. Suh, D. Majumdar, and K. S. Kim, *J. Chem. Phys.* **113**, 5259 (2000).
- [82] B. Santra, A. Michaelides, M. Fuchs, A. Tkatchenko, C. Filippi, and M. Scheffler, *J. Chem. Phys.* **129**, 194111 (2008).
- [83] T. L. Beck, M. E. Paulaitis, and L. R. Pratt, *The Potential Distribution Theorem and Models of Molecular Solutions* (Cambridge, New York, 2006).
- [84] A. J. Misquitta, R. Podeszwa, B. Jeziorski, and K. Szalewicz, *J. Chem. Phys.* **123**, 214103 (2005).
- [85] R. Bukowski, K. Szalewicz, G. C. Groenenboom, and A. van der Avoird, *Science* **315**, 1249 (2007).
- [86] D. Asthagiri and L. R. Pratt, *Chem. Phys. Lett.* **371**, 613 (2003).
- [87] D. Asthagiri, L. R. Pratt, and H. S. Ashbaugh, *J. Chem. Phys.* **119**, 2702 (2003).
- [88] S. Varma and S. B. Rempe, *J. Am. Chem. Soc.* **130**, 15405 (2008).